This is an open access article published under an ACS AuthorChoice License, which permits copying and redistribution of the article or any adaptations for non-commercial purposes.

ACS OMEGA

Article

Cite This: ACS Omega 2019, 4, 12366−12374

http://pubs.acs.org/journal/acsodf

Magnetofection of Green Fluorescent Protein Encoding DNA-Bearing Polyethyleneimine-Coated Superparamagnetic Iron Oxide Nanoparticles to Human Breast Cancer Cells

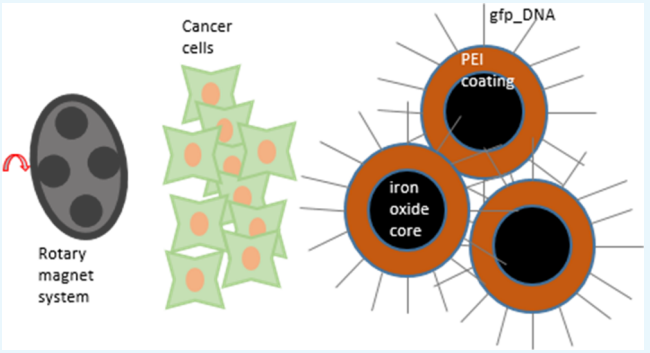
Merve Zuvin,[†] Efe Kuruoglu,[†] Veysel Ogulcan Kaya,[‡] Ozlem Unal,[∥] Ozlem Kutlu,[§,⊥] Havva Yagci Acar,[§,∥] Devrim Gozuacik,[‡,§,⊥] and Ali Koşar*[,†,§,⊥]

[†]Mechatronics Engineering Program, Faculty of Engineering and Natural Sciences, [‡]Molecular Biology, Genetics and Bioengineering Program, Faculty of Engineering and Natural Sciences, and [§]Center of Excellence for Functional Surfaces and Interfaces for Nano Diagnostics (EFSUN), Sabanci University, Orhanli, 34956 Tuzla, Istanbul, Turkey

[∥]Department of Chemistry, Faculty of Arts and Sciences, Koc University, 34450 Sariyer, Istanbul, Turkey

[⊥]SUNUM Nanotechnology Research and Application Center, Orhanli, 34956 Tuzla, Istanbul, Turkey

ABSTRACT: Gene therapy is a developing method for the treatment of various diseases. For this purpose, the search for nonviral methods has recently accelerated to avoid toxic effects. A strong alternative method is magnetofection, which involves the use of superparamagnetic iron oxide nanoparticles (SPIONs) with a proper organic coating and external magnetic field to enhance the localization of SPIONs at the target site. In this study, a new magnetic actuation system consisting of four rare-earth magnets on a rotary table was designed and manufactured to obtain improved magnetofection. As a model, green fluorescent protein DNA-bearing polyethyleneimine-coated SPIONs were used. Magnetofection was tested on MCF7 cells. The system reduced the transfection time (down to 1 h) of the standard polyethyleneimine transfection protocol. As a result, we showed that the system could be effectively used for gene transfer.



INTRODUCTION

Gene therapy is defined as insertion of an exogenous gene into cells to compensate for the abnormal gene or to make beneficial proteins, for example, to affect the immune system or angiogenesis.[1−6] The exogenous gene needs to be transported to the cell in vectors, which are classified as viral and nonviral vectors. Commonly used viral vectors are the adenovirus, lentivirus, and adeno-associated viruses.[7−9] While viral vectors are efficient carriers, they pose potential risks. On the other hand, nonviral vectors emerged as a safer alternative. Cationic lipids and polymers are commonly used nonviral vectors.[10] They are regarded as suitable carriers for genes in the free form or in the form bound to nanoparticles.[11,12] Magnetic nanoparticles are strong candidates for this task.[13−15] Superparamagnetic iron oxide nanoparticles are quite popular in magnetic resonance imaging for diagnosis and also for drug/gene delivery as therapeutics for various diseases because of their biocompatibility in addition to magnetic properties.[16−19]

Transferring magnetic nanoparticle-bound genes into target cells/tissues using a magnetic field is called magnetofection.[20−22] Such nanoparticles are generally coated with cationic polymers for DNA binding. Then, they interact with the cell membrane and are dispersed into the cytoplasm through endosomal escape. In this case, the particles remain in cellular vesicles and are taken up by endocytosis. After internalization by the cells, DNA is released via a proton sponge effect.[20,23,24] Polyethyleneimine (PEI) is the conventional and well-established transfection agent. However, it is known to be toxic, limiting the applicable dose.[19,21] Binding PEI on magnetic nanoparticles and using a magnetic field increase the transfection efficiency while reducing the toxicity.[17,25]

In our previous study, we showed that polyethyleneimine-coated superparamagnetic nanoparticles (PEI-SPIONs) can efficiently transfer green fluorescent protein encoding DNA (GFP-DNA) under varying magnetic fields.[26] In an 8 h magnetofection procedure, viability improved, but the transfection efficiency was below the standard PEI transfection method.

In this study, alterations, which could be introduced to the standard PEI transfection protocol, were investigated using MCF7 cells reported as resistant to transfection.[26] Accordingly, the transfection time of 8 h was reduced to 1 h after inspecting transfection efficiencies for 3 h. When the transfection

Received: April 8, 2019
Accepted: July 4, 2019
Published: July 18, 2019

Downloaded via KOC UNIV on October 10, 2019 at 12:47:26 (UTC).
See https://pubs.acs.org/sharingguidelines for options on how to legitimately share published articles.

efficiencies were examined, we proved that efficient transfection could be performed even within a short time (1 h) with the developed new generation actuation system. Accordingly, GFP-DNA transfer to the MCF7 cell line with high efficiency was achieved with magnetofection. The new actuation system was designed for overcoming the toxicity effect of the standard PEI transfection protocol with an improved efficiency. Hence, the feasibility for replacing the standard PEI transfection protocol was investigated and presented.

RESULTS AND DISCUSSION

Actuation System. A varying magnetic field was generated by rotating the system consisting of four magnets on a plexiglass table as shown in Figure 1. Each individual magnet had a magnetic field flux of 230 mT. The magnetic flux values of the system were utilized in the numerical model with air as the ambient (Figure 2a). The system was modeled to prove the nonuniform magnetic field distribution throughout the rotary table.

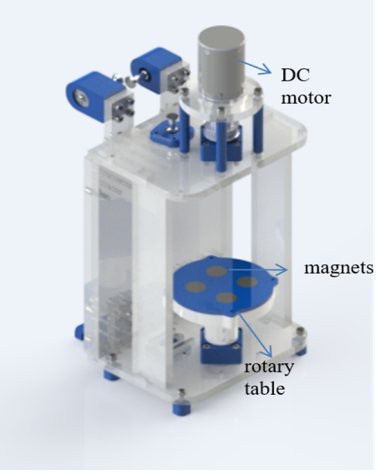


Figure 1. Magnetic actuation system. (This photo is taken by the lead author Merve Zuvin.)

Simulations were performed using a workstation of Intel Core i7-3630QM CPU with a 2.40 GHz processor. The diameter and thickness of the magnets were 2.5 cm and 0.5 cm, respectively (Figure 2b). The plexiglass table was 9 cm wide and 0.5 cm thick. An extremely fine free tetrahedral mesh configuration (1151002 domain, 33178 boundary, and 1072 edge elements) was used (Figure 2c,d). The governing equations are as follows:

$$\nabla x H = J \tag{1}$$

$$\nabla x A = B \tag{2}$$

$$\sigma E = J \tag{3}$$

Here, H is the magnetic field strength, B is the magnetic field, and A is magnetic vector potential (25). J is the current (in our case, it is 0), E is the electric field (in our case is 0), and σ is the electrical conductivity. The magnetic field flux value of the magnet system was utilized in multiphysics software COMSOL5.2a using a configuration of four magnets and a plexiglass table for magnets.

According to the simulation results, the maximum magnetic force values are obtained at a distance of 2 cm from the rotary table (Figure 3a). Furthermore, as the distance between the sample and the magnet system increases, the magnetic force decreases. However, the fluxes exerted from magnets are distributed in such a way that their magnetic forces move in a circular pattern around the center of these four magnets. Thus, the circulating effect initiates at the distance of 2.5 cm (Figure 3b), and it leads to neither small forces at larger distances nor forces concentrated at shorter distances. At the distances of 3 and 3.5 cm, less-concentrated magnetic patterns are observed, and smaller forces are generated (Figure 3c–e). All the magnetic flux density patterns regarding Figure 3a–e are combined to a single 3D illustration (Figure 3f).

Because of a strong magnetic field observed in the light of the findings of simulations, 2, 2.5, 3, and 3.5 cm distances are examined for the cell experiments. The objective of the rotating system is to allow as many nanoparticles as possible to enter into the cells, which are attached to the plate.

The system generated a nonuniform magnetic field with fluxes varying from 2 to 60 mT through the rotary table, which were experimentally measured. To visualize the effect of distance between the sample and rotary table, iron dust particles were used. It can be observed that iron dust particles are influenced by the magnets' own fields and aggregate on individual magnets as expected when the petri dish containing iron dusts is placed on the magnets and cluster near the edges (Figure 4a). When the petri dish is slowly removed upward (from the table), the magnets work together, and the dust particles are evenly distributed in the plate (Figure 4b). Then, the effect of the rotation of the system on dusts is investigated. Accordingly, when the behavior of dust particles at different distances is examined, it can be seen that, for a 2.5 cm distance, dust particles arrange successively, and the particles are continuously lifted from one side and roll around the center (Figure 4c–f). In a permanent magnetic actuation system, the particles experience a lifting force given as

$$F = \frac{\mu_0 M^2 A}{2} = \left(\frac{(\mu_0 M)^2 A}{2\mu_0}\right) \tag{4}$$

where F is the lifting force of a permanent magnet, μ_0 is the magnetic permeability $4\pi \times 10^{-7}$ N/A^2 , M is the magnetization, $\mu_0 M$ is the saturation magnetization, and A is the area of magnetization (area of rotary table) [26]. In our system, the saturation magnetization of a single magnet is 230 mT, while the generated lifting force is 971.26 kN. These results provide clues for particle motion under magnetic field application in the system for cell experiments.

Cell Experiments. The cell experiments were carried out with three different samples, namely, polyethyleneimine (PEI), polyethyleneimine-coated superparamagnetic iron oxide nanoparticles without a magnetic field (PS w/o mag), and polyethyleneimine-coated superparamagnetic iron oxide nanoparticles under rotary magnetic fields (PS rot mag), and a single dose of 60 μg of PEI (both free and bound). First, the effect of distances is investigated. Figure 5 illustrates the experimental procedure steps.

In order to obtain a uniform distribution, 2, 2.5, 3, and 3.5 cm distances are explored based on the findings of numerical simulations. After the experiments, the transfection efficiencies and cell viability are examined (Figure 6). PEI and PS w/o mag (PEI-SPION without magnetic field exposure) were used as control and treated in the same way as their counterparts. PS rot mag indicates PEI-SPION exposed to rotary magnetic fields.

DOI: 10.1021/acsomega.9b01000
ACS Omega 2019, 4, 12366−12374

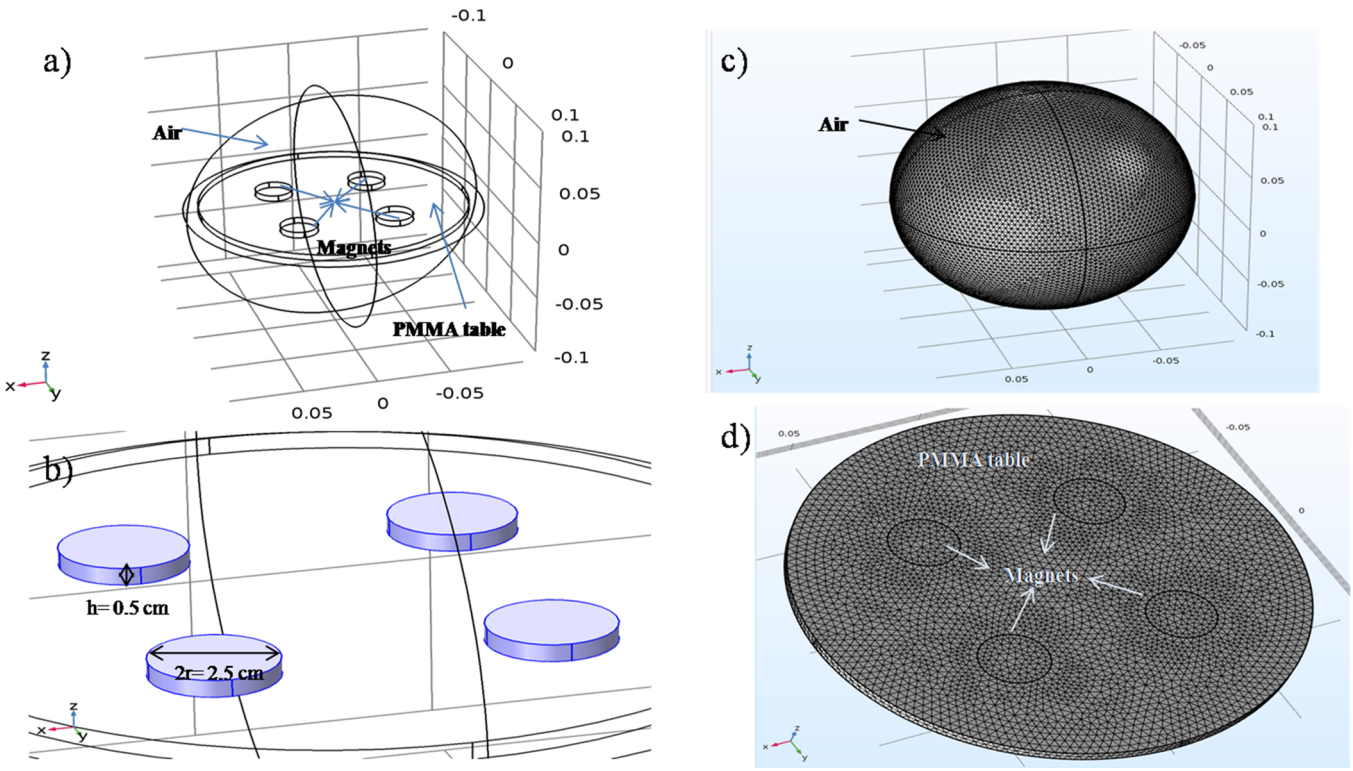


Figure 2. Model of the study: (a) modeling setup, (b) sizes of magnets, (c) general view of the mesh configuration, and (d) close-up view of the mesh configuration

According to the results, a 60 rpm velocity is enough to obtain efficient transfection, and the distance is found to be an important parameter for cell viability. Since the magnetic field effect is stronger at shorter distances (2 and 2.5 cm), the number of dead cells is high. Compared to that of 2 and 2.5 cm, the viability is improved at distances of 3 and 3.5 cm. However, the 3.5 cm distance leads to a higher transfection efficiency compared to the 3 cm. (Figure 6). Thus, 3.5 cm is chosen as the optimum distance, and the magnetofection effect is further investigated at different times (Figure 7). pDNA only, PEI, and PS w/o mag (PEI-SPION without magnetic field exposure) were used as control and treated in the same way as their counterparts. PS rot mag indicates PEI-SPION exposed to rotary magnetic fields.

At 2 h of experiment, transfection efficiency is low, while it increased at 4 h. However, at this time point, magnetic field exposure for 2 h decreases the cell viability (Figure 7). Therefore, at a 3.5 cm distance, 1 h of transfection time is investigated, and further enhancement of cell viability and efficient transfection can be achieved (Figure 8a–f). According to results, 1 h of the transfection efficiency of PEI remained low (approximately 2%), while that of PS rot mag at 3.5 cm is approximately 50% (Figure 8). Therefore, we could achieve high transfection efficiency as well as improved viability by using PEI-coated SPIONs exposed to the rotary magnetic field. The utilization of only PEI results in improved viability but failed transfection.

Many different magnetic systems are being used for gene transfer. The popular ones are oscillating magnet arrays, placing magnets under culture plates and magnet arrays.[25,27,28] McBain et al.[27] used an oscillating magnet array and reported that human lung epithelial cells were effectively transfected. They reported positive effects of the system on viability. In our study, magnetic field application significantly raised the viability. In addition, the transfection time was reduced to 1 h since all the transfection agents were removed from the cells at the end of 1 h.

Lu et al.[28] used a staggered magnet array and placed two magnets underneath the culture plates. Two adjacent magnets interfered with each other and had a negative effect on transfection. Because the two magnets were affected by each other, they claimed that the efficiency was more in between them. Accordingly, the cells, which were located above the magnets, experienced a uniform magnetic field, while the cells in the other wells of the plate were exposed to nonuniform magnetic fields. The group concluded that the nonuniform magnetic field was more suitable for in vivo studies. However, in our system, we benefit from the condition of the interaction of two magnets with each other. A uniform transfection could be obtained under a nonuniform magnetic field by finding the appropriate distance between the magnets and culture plate (Figure 2b). Cell experiments at various distances were performed for this task. At the smallest distance of 2 cm, a more concentrated cell population was seen around the magnet, and a cell population was found distributed throughout the entire 10 cm plate at the 3.5 cm distance.

PEI is an effective agent for transfection. Some studies with PEI reported that free PEI is needed for high transfection efficiencies, and its effects on transfection were investigated.[23] The results showed that nanoparticles could not enter into the cell nucleus but free PEI in the medium helped in sending the plasmids to the nucleus. In other words, since a sufficient number of nanoparticles could not be directed to the core, excessive PEI was concentrated in the cell. Therefore, it is important that the cells should be in contact with PEI for short periods and in sufficient quantities. Although PEI is a well-

DOI: 10.1021/acsomega.9b01000
ACS Omega 2019, 4, 12366−12374

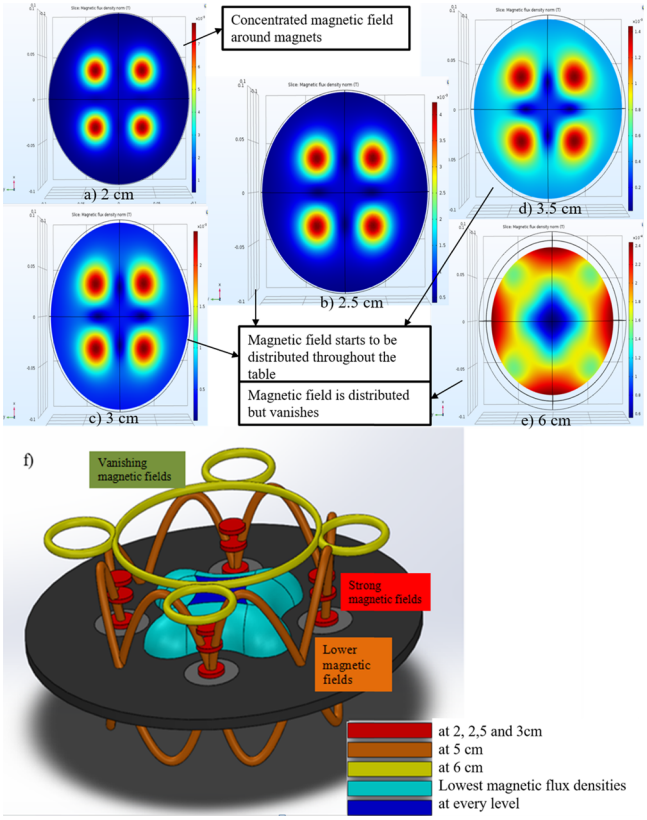


Figure 3. Simulation results and 3D magnetic flux density norm patterns of the magnetic system: (a) The maximum magnetic force occurs at the distance of 2 cm; (b) at the distance of 2.5 cm, distribution starts; (c, d) a nonconcentrated magnetic force is observed at the distances of 3 and 3.5 cm; (e) at the distance of 6 cm, magnetic fluxes are combined into a circular pattern, and the magnetic force significantly decreases. (f) The red line represents densities at the distances of 2, 2.5, and 3 cm; orange and yellow ones correspond to the distances of 5 and 6 cm, respectively; light and dark blue represent the lowest magnetic flux density at every level.

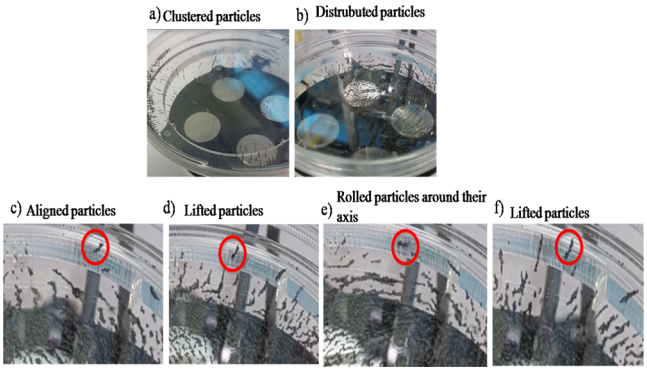


Figure 4. Iron dust particle experiments: (a) under a uniform magnetic field, dust particles cluster near the magnets and edges; (b) under a nonuniform magnetic field, dusts begin to distribute throughout the plate when the system is operational; (c) dusts align successively, (d) lift, (e) roll, and change direction in their own axis and then (f) lift again.

established effective transfection agent, the toxicity of the material is a known fact.[29] Some studies showed that using PEI-coated SPIONs for transfection leads to less toxicity and improved efficiencies compared to the use of only PEI.[30,31]

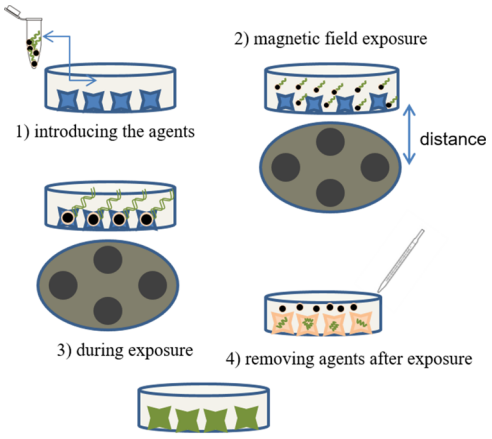


Figure 5. Experimental procedure. Schematic representation of experimental steps: (1) introducing the agents, (2) magnetic field exposure, (3) during exposure, (4) removing agents after the procedure, and (5) after expression.

Moreover, Lipofectamine is another reagent also widely used for transfection of cells with a very similar experimental protocol of PEI. However, the main difference between Lipofectamine and PEI is their mechanism of action on the cell membrane. Lipofectamine creates DNA-encapsulated liposomes, and these liposomes fuse with the cell membrane and thus release the DNA into the cytoplasm.[32] On the other hand, in PEI transfection, the cationic polymer interacts with the cell membrane so that DNA is introduced to the cell via endocytosis.[33] Although some studies use Lipofectamine as a control, in most of the PEI-mediated magnetofection studies, free PEI is used as a common control of its nanoformulated versions.[30,31,34−36] Accordingly, in our experimental setup, we investigate the effect of magnetofection by applying a cationic polymer-based transfection procedure using PEI-coated SPIONs. Therefore, we use free PEI rather than lipofectamine. The nanoparticles were sent to the cells with a total amount of 60 μg of PEI-bearing nanoparticle solution, and the transfection times were changed while ensuring the sufficiency of the amount used in the experiments. In addition, when the duration of transfection is short, the efficiency of the transfection by PEI-SPION nanoparticles is still significant because the capability of the actuation system while using only PEI fails in achieving transfection to the cells. Moreover, the use of PEI-coated SPION nanoparticles was not associated with toxicity as we reported in our previous study.[26]

Huth et al. examined the nanoparticle uptake of HeLa cells.[37] They found that the PEI-coated nanoparticles were close to the cell membrane at the 5th minute, on the cell surface at the 10th minute, and in the cell at the 15th minute. Motivated by this finding, the purpose of our study is benefitting from a rotating, that is, nonuniform, magnetic field to allow more particles to enter the cell, thereby increasing the number of particles the cell can encounter. In this regard, we prove that efficient transfection could be obtained in a short time.

Accordingly, efficient transfection can be achieved using nanoparticles with our new generation actuation system even within a 1 h period where standard PEI transfection was not successful. Thus, the viability could be increased, and gene transfer would be efficient.

DOI: 10.1021/acsomega.9b01000
ACS Omega 2019, 4, 12366−12374

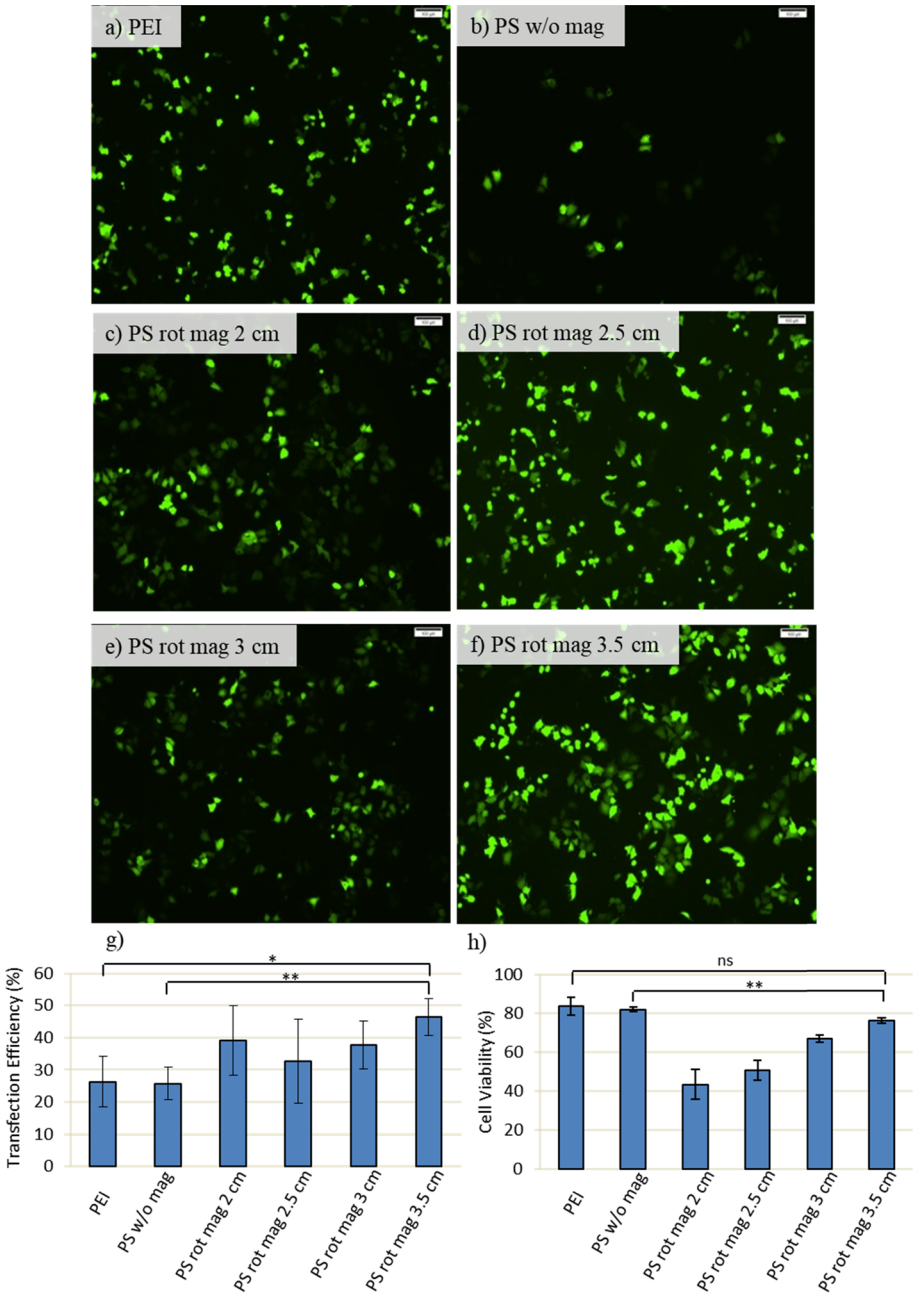


Figure 6. Transfection efficiency and cell viability with respect to variable distance: MCF7 cells are transfected with 60 μg of PEI (polyethyleneimine) or PS (PEI-coated superparamagnetic iron oxide nanoparticles (SPION)) together with 10 μg of GFP-DNA and then exposed to a magnetic field for 1 h. After incubation of cells at 37 °C for an additional 2 h, transfection solutions are removed by washing with PBS, and the culture was maintained in fresh DMEM medium until incubation time is achieved to 48 h. (a–f) GFP expression is observed by inverted fluorescence microscopy at 48 h post-transfection. Scale bar: 100 μm. (g) Quantification of transfection efficiency analyzed by counting at least 900 cells for each condition. (h) Cell viability obtained by MTT assay. Cells are treated for 4 h with 0.5 mg/mL MTT in complete medium. Then, the absorbance of formazan solution is measured by using enzyme-linked immunosorbent assay. PEI and PS w/o mag (PEI-SPION without magnetic field exposure) were used as control and treated in the same way as their counterparts. PS rot mag indicates PEI-SPION exposed to rotary magnetic fields. Data were shown as mean ± SD of at least 3 independent experiments; ns: nonsignificant, *$p < 0.05$, **$p < 0.01$.

Due to their adverse effects, viral and nonviral chemical vectors should not be favored in gene therapy. In addition to their biosafety problems, such vectors have a limited amount of access for transporting exogenous DNA. Accordingly, research outputs in nanotechnology recommend new techniques such as using magnetic nanoparticles in gene therapy, especially in transfection, which could be ensured with our actuation system.

CONCLUSIONS

Due to many advantages such as manipulation capability and less toxicity, their utilization in biotechnology has an increasing trend. In this study, we presented a magnetic actuation system for transfection and GFP-DNA transfer to MCF7 cells with PEI-SPION carriers. The results showed that the magnetic field exposure increased the transfection efficiency with nanoparticles while maintaining the viability. At an optimum distance for a cell culture plate with a diameter of 10 cm, a

DOI: 10.1021/acsomega.9b01000
ACS Omega 2019, 4, 12366−12374

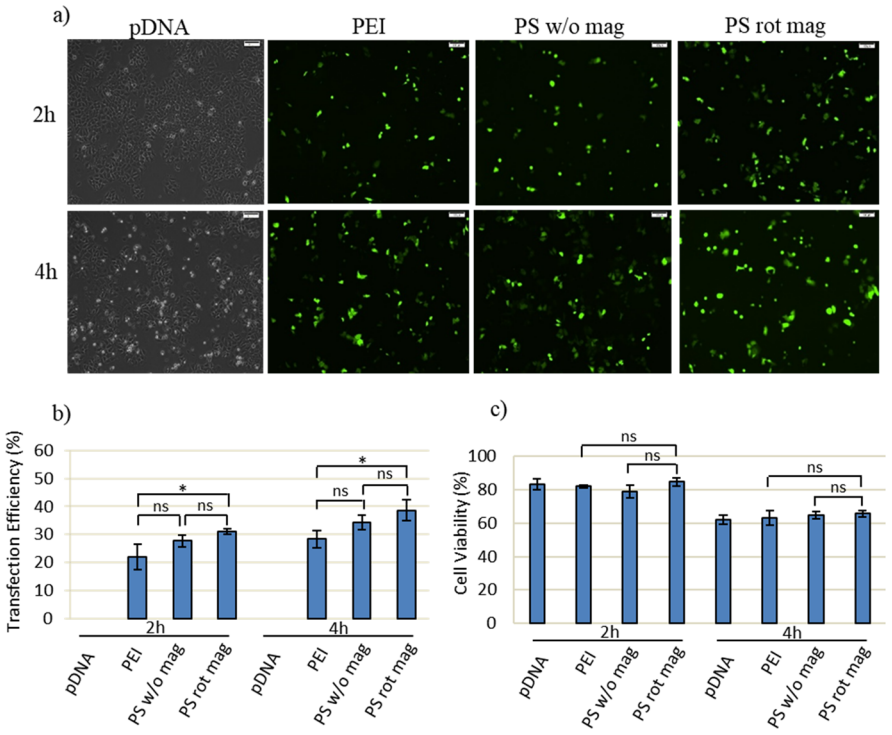


Figure 7. Transfection efficiency and viability assay at a 3.5 cm distance with respect to different times. MCF7 cells are transfected with 60 μg of PEI or PS together with 10 μg of GFP-DNA. For the 2 h experiment, cells are exposed to the magnetic field for 1 h and then incubated at 37 °C for the additional 1 h. For the 4 h experiment, cells are exposed to the magnetic field for 2 h and then incubated at 37 °C for the additional 2 h. In both cases, transfection solutions are removed after incubation by washing with PBS, and the culture is maintained in fresh DMEM medium until incubation time is achieved to 48 h. (a) GFP expression is observed by inverted fluorescence microscopy at 48 h post-transfection. Scale bar: 100 μm. (b) Quantification of transfection efficiency analyzed by counting at least 900 cells for each condition. (c) Cell viability obtained by MTT assay. Cells are treated for 4 h with 0.5 mg/mL MTT in complete medium. Then, the absorbance of formazan solution is measured by using enzyme-linked immunosorbent assay. pDNA only, PEI, and PS w/o mag (PEI-SPION without magnetic field exposure) were used as control and treated in the same way as their counterparts. PS rot mag indicates PEI-SPION exposed to rotary magnetic fields. Data were shown as mean ± SD of at least 3 independent experiments; ns: non-significant, $*p < 0.05$.

uniform magnetic field distribution was obtained, and efficient in vitro gene transfer was achieved. The system, which is developed in this study, enables an efficient transfection within a short time and could be easily tested in both vitro and in vivo studies.

MATERIALS AND METHODS

Cells and Reagents. The pmax-GFP mammalian expression vector was supplied by Amaxa (Amaxa, Lonza, Switzerland). Branched PEI (MW 25,000) was purchased from Sigma-Aldrich (408727-USA). Dulbecco's modified Eagle's medium (DMEM) was purchased from Sigma-Aldrich (D5671-Germany). L-Glutamine (BIO3-020-1B), penicillin/streptomycin (BIO3-031-1B), and trypsin−EDTA (BIO3-050-1A) were purchased from Biological Industries (Israel). Fetal bovine serum (FBS) was purchased from BioWest (S1810-USA). Phosphate buffered saline (PBS-17-516F) without calcium or magnesium was purchased from Lonza (U.S.A.). The breast cancer (MCF-7, HTB-22) cell line was obtained from American Type Culture Collection (ATCC, U.S.A.).

Magnetic Actuation System. The system consists of a rotary table, which has four rare-earth magnets, a 12 V DC motor, power cables, and adjustable plexiglass stages for placing 10 cm petri dishes (Figure 1). The magnets were placed in such a way that their poles pulled each other. Rotation of the table was provided with the 12 V DC motor. The parts of the system were fabricated with the laser cutting and 3D printing techniques. Magnetic field fluxes of the magnets and the variation of the magnetic field depending on the distance between table and sample were measured by a gaussmeter (Hirst Magnetic Instruments Ltd.). The system was also modeled via the ac/dc module of the COMSOL Multiphysics 5.2a software for simulating the magnetic fluxes exerted on the sample.

PEI-SPION Synthesis and Characterization. PEI-coated SPIONs were prepared by a ligand exchange method as explained in our previous work.[26] This sample was directly used for DLS (dynamic light scattering) and zeta potential measurements. Atomic force microscopy (AFM) analysis was performed on a Bruker Dimension Icon in the ScanAsyst mode in air with ScanAsyst-Air cantilever (Bruker, U.S.A., k = 0.4 N/m, frequency = 70 kHz). The samples were diluted with ethanol, sonicated, and drop-cast on a silicon wafer for analysis. Eighty percent of the total product mass (PEI-SPION) was determined as PEI by thermogravimetric analysis performed on dried samples.

Plasmid DNA Isolation. Plasmid DNA isolation was performed with a plasmid DNA purification kit according to manufacturer's instructions (Nucleobond Xtra Midi/Maxi, Macherey-Nagel, Germany).

Cell Culture. MCF-7 human breast cancer cells were cultured in DMEM supplemented with 10% fetal bovine serum (FBS) and antibiotics (Penicillin−Streptomycin). Cells (1.2×10^6) were seeded on 10 cm culture plates in a 10 mL cell

DOI: 10.1021/acsomega.9b01000
ACS Omega 2019, 4, 12366−12374

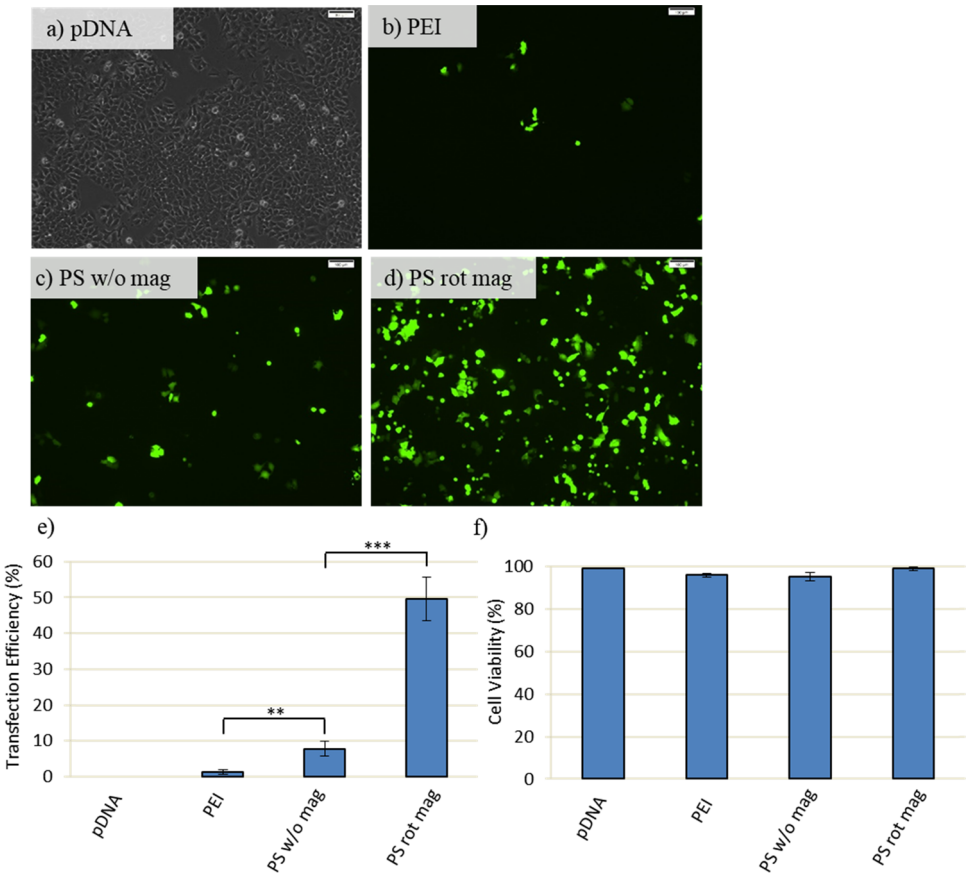


Figure 8. Transfection efficiency and viability assay at 3.5 cm distance and 1 h: MCF7 cells are transfected with 60 μg of PEI or PS together with 10 μg of GFP-DNA. Following transfection, cells are exposed to the magnetic field for 1 h and then washed with PBS right after magnetofection to remove uninternalized nanoparticles. Cells are incubated at 37 °C in fresh DMEM medium until incubation time is achieved to 48 h. (a–d) GFP expression is observed by inverted fluorescence microscopy at 48 h post-transfection. Scale bar: 100 μm. (e) Quantification of transfection efficiency analyzed by counting at least 900 cells for each condition. (f) Cell viability obtained by MTT assay. Cells are treated for 4 h with 0.5 mg/mL MTT in complete medium. Then, the absorbance of formazan solution is measured by using enzyme-linked immunosorbent assay. pDNA only, PEI, and PS w/o mag (PEI-SPION without magnetic field exposure) were used as control and treated in the same way as their counterparts. PS rot mag indicates PEI-SPION exposed to rotary magnetic fields. Data were shown as mean ± SD of at least 3 independent experiments; $^{**}p < 0.01$, $^{***}p < 0.001$.

culture medium. Cells were incubated at 37 °C in a humidified incubator with a 5% CO_2 atmosphere.

Magnetofection. Sixty micrograms of 25 kDa branched PEI (as control) or PEI-SPION solutions, which carried 60 μg of 25 kDa branched PEI, was added into Eppendorf tubes containing 200 μL of DMEM (without serum and antibiotics). In another Eppendorf tube, 10 μg of plasmid DNA (pDNA)-encoding GFP was mixed with 200 μL DMEM (without serum and antibiotics). To allow binding of DNA to PEI and PEI-SPION particles, the transfection mixture is incubated for 10 min at room temperature and then added dropwise onto the culture plates. pDNA alone is used as a negative control of transfection. For magnetofection experiments, cells were exposed to the magnetic field for 1 h or 2 h and incubated for an additional 1 h or 2 h at 37 °C in the presence of the transfection agent. Then, the transfection agent is removed by washing with PBS, and cells are cultured in fresh DMEM medium until total incubation time is achieved to 48 h. In another set, cells were washed right after 1 h magnetofection to remove the uninternalized nanoparticles, fresh medium is added, and cells are again cultured for 48 h. For experiments without the magnetic field (PEI control, PS w/o mag), the same steps were carried out except for the magnetic field exposure.

Microscopy Analysis and Transfection Efficiency. At 48 h post-transfection, transfection efficiency was determined using an inverted fluorescent microscope (Olympus IX70) with 10× magnification. About 900 cells were counted for each sample.

Cell Viability Assays. Cells transfected with PEI or PEI-SPION in the presence or absence of rotating magnetic field conditions were harvested at 48 h post-transfection, and viability was assessed by a mitochondrial function-based MTT [3-(4,5-dimethylthiazol-2yl)-2,5-diphenyltetrazolium bromide] assay as described previously.[29,30] Briefly, cells were incubated for 4 h with 0.5 mg/mL MTT in complete medium. The medium was then aspirated, and cells were lysed with DMSO to dissolve formazan crystals. MTT is a yellow tetrazolium salt reducing to purple formazan. The absorbance of formazan solution was measured on an enzyme-linked immunosorbent assay (ELISA) plate reader (iMark Microplate Reader, Bio-Rad) at wavelengths of 570 and 655 nm.

Statistical Analysis. Statistical analyses were performed using one-way ANOVA for multiple comparisons and the Student's t test for intergroup comparison. Data were

DOI: 10.1021/acsomega.9b01000
ACS Omega 2019, 4, 12366−12374

represented as means ± SD of at least three independent experiments. Values of $p < 0.05$ were considered statistically significant.

AUTHOR INFORMATION

Corresponding Author

*E-mail: kosara@sabanciuniv.edu.

ORCID

Devrim Gozuacik: 0000-0001-7739-2346

Ali Koşar: 0000-0001-6283-6717

Notes

The authors declare no competing financial interest.

ACKNOWLEDGMENTS

The authors would like to thank the Sabanci University Nanotechnology Research and Application Center (SUNUM) and Koc University Surface Science and Technology Center (KUYTAM) for the continued equipment and characterization support. This work was supported by the Turkish Scientific Council (TUBITAK), grant number 213 M669, Koc University, and Turkish Academy of Sciences. D.G. is a recipient of the EMBO-SDIG Award. A.K. received the TUBITAK Incentive Award. D.G. and A.K. are recipients of the Turkish Academy of Sciences (TUBA-GEBIP) Award. H.Y.A received National L'Oréal Women in Science Reward in Materials Science.

ABBREVIATIONS

pDNA	plasmid DNA
SPION	superparamagnetic iron oxide nanoparticle
PEI	Polyethyleneimine
PS	PEI-SPION
PS w/o mag	PEI-SPION without magnetic field
PS rot mag	PEI-SPION with rotary magnetic field
GFP	green fluorescent protein
MCF7	human breast cancer cell line
DMEM	Dulbecco's modified Eagle's medium

REFERENCES

(1) Curtin, C. M.; Tierney, E. G.; Mcsorley, K.; Cryan, S.-A.; Duffy, G. P.; O'Brien, F. J. Combinatorial Gene Therapy Accelerates Bone Regeneration: Non-Viral Dual Delivery of VEGF and BMP2 in a Collagen-Nanohydroxyapatite Scaffold. *Adv. Healthcare Mater.* **2015**, *4*, 223−227.

(2) Jackson, K. L.; Dayton, R. D.; Orchard, E. A.; Ju, S.; Ringe, D.; Petsko, G. A.; Maquat, L. E.; Klein, R. L. Preservation of Forelimb Function by UPF1 Gene Therapy in a Rat Model of TDP-43-Induced Motor Paralysis. *Gene Ther.* **2015**, *22*, 20−28.

(3) Mangraviti, A.; Tzeng, S. Y.; Kozielski, K. L.; Wang, Y.; Jin, Y.; Gullotti, D.; Pedone, M.; Buaron, N.; Liu, A.; Wilson, D. R.; et al. Polymeric Nanoparticles for Nonviral Gene Therapy Extend Brain Tumor Survival in Vivo. *ACS Nano* **2015**, *9*, 1236−1249.

(4) Georgiadis, A.; Duran, Y.; Ribeiro, J.; Abelleira-Hervas, L.; Robbie, S. J.; Sünkel-Laing, B.; Fourali, S.; Gonzalez-Cordero, A.; Cristante, E.; Michaelides, M.; et al. Development of an Optimized AAV2/5 Gene Therapy Vector for Leber Congenital Amaurosis Owing to Defects in RPE65. *Gene Ther.* **2016**, *23*, 857−862.

(5) Li, T.; Kang, G.; Wang, T.; Huang, H. Tumor Angiogenesis and Anti-Angiogenic Gene Therapy for Cancer (Review). *Oncol. Lett.* **2018**, *16*, 687−702.

(6) Marelli, G.; Howells, A.; Lemoine, N. R.; Wang, Y. Oncolytic Viral Therapy and the Immune System: A Double-Edged Sword against Cancer. *Front. Immunol.* **2018**, *9*, 866.

(7) Palfi, S.; Gurruchaga, J. M.; Ralph, G. S.; Lepetit, H.; Lavisse, S.; Buttery, P. C.; Watts, C.; Miskin, J.; Kelleher, M.; Deeley, S.; et al. Long-Term Safety and Tolerability of ProSavin, a Lentiviral Vector-Based Gene Therapy for Parkinson's Disease: A Dose Escalation, Open-Label, Phase 1/2 Trial. *Lancet* **2014**, *383*, 1138−1146.

(8) Crystal, R. G. Adenovirus: The First Effective In Vivo Gene Delivery Vector. *Hum. Gene Ther.* **2014**, *25*, 3−11.

(9) MacLaren, R. E.; Groppe, M.; Barnard, A. R.; Cottriall, C. L.; Tolmachova, T.; Seymour, L.; Reed Clark, K.; During, M. J.; Cremers, F. P. M.; Black, G. C. M.; et al. Retinal Gene Therapy in Patients with Choroideremia: Initial Findings from a Phase 1/2 Clinical Trial. *Lancet* **2014**, *383*, 1129−1137.

(10) Agrawal, P.; Ingle, N. P.; Boyle, W. S.; Ward, E.; Tolar, J.; Dorfman, K. D.; Reineke, T. M. Fast, Efficient, and Gentle Transfection of Human Adherent Cells in Suspension. *ACS Appl. Mater. Interfaces* **2016**, *8*, 8870−8874.

(11) Ramamoorth, M.; Narvekar, A. Non Viral Vectors in Gene Therapy - An Overview. *J. Clin. Diagn. Res.* **2015**, *9*, GE01−GE06.

(12) Yin, H.; Kanasty, R. L.; Eltoukhy, A. A.; Vegas, A. J.; Dorkin, J. R.; Anderson, D. G. Non-Viral Vectors for Gene-Based Therapy. *Nat. Rev. Genet.* **2014**, *15*, 541−555.

(13) Elsherbini, A. A. M.; Saber, M.; Aggag, M.; El-Shahawy, A.; Shokier, H. A. A. Magnetic Nanoparticle-Induced Hyperthermia Treatment under Magnetic Resonance Imaging. *Magn. Reson. Imaging* **2011**, *29*, 272−280.

(14) Loh, X. J.; Lee, T.-C.; Dou, Q.; Deen, G. R. Utilising Inorganic Nanocarriers for Gene Delivery. *Biomater. Sci.* **2016**, *4*, 70−86.

(15) Majidi, S.; Zeinali Sehrig, F.; Samiei, M.; Milani, M.; Abbasi, E.; Dadashzadeh, K.; Akbarzadeh, A. Magnetic Nanoparticles: Applications in Gene Delivery and Gene Therapy. *Artif. Cells, Nanomed,, Biotechnol.* **2016**, *44*, 1186−1193.

(16) Eslaminejad, T.; Noureddin Nematollahi-Mahani, S.; Ansari, M. Glioblastoma Targeted Gene Therapy Based on PEGFP/P53-Loaded Superparamagnetic Iron Oxide Nanoparticles. *Curr. Gene Ther.* **2017**, *17*, 59−69.

(17) Uthaman, S.; Lee, S. J.; Cherukula, K.; Cho, C.-S.; Park, I.-K. Polysaccharide-Coated Magnetic Nanoparticles for Imaging and Gene Therapy. *BioMed Res. Int.* **2015**, 959175.

(18) Xiao, S.; Castro, R.; Rodrigues, J.; Shi, X.; Tomás, H. PAMAM Dendrimer/PDNA Functionalized-Magnetic Iron Oxide Nanoparticles for Gene Delivery. *J. Biomed. Nanotechnol.* **2015**, *11*, 1370−1384.

(19) Stephen, Z. R.; Dayringer, C. J.; Lim, J. J.; Revia, R. A.; Halbert, M. V.; Jeon, M.; Bakthavatsalam, A.; Ellenbogen, R. G.; Zhang, M. Approach to Rapid Synthesis and Functionalization of Iron Oxide Nanoparticles for High Gene Transfection. *ACS Appl. Mater. Interfaces* **2016**, *8*, 6320−6328.

(20) Wahajuddin; Arora, S. Superparamagnetic Iron Oxide Nanoparticles: Magnetic Nanoplatforms as Drug Carriers. *Int. J. Nanomed.* **2012**, *7*, 3445−3471.

(21) Scherer, F.; Anton, M.; Schillinger, U.; Henke, J.; Bergemann, C.; Krüger, A.; Gänsbacher, B.; Plank, C. Magnetofection: Enhancing and Targeting Gene Delivery by Magnetic Force in Vitro and in Vivo. *Gene Ther.* **2002**, *9*, 102−109.

(22) Plank, C.; Scherer, F.; Schillinger, U.; Bergemann, C.; Anton, M. Magnetofection: Enhancing and Targeting Gene Delivery with Superparamagnetic Nanoparticles and Magnetic Fields. *J. Liposome Res.* **2003**, *13*, 29−32.

(23) Zhang, L.; Li, Y.; Yu, J. C.; Chen, Y. Y.; Chan, K. M. Assembly of Polyethylenimine-Functionalized Iron Oxide Nanoparticles as Agents for DNA Transfection with Magnetofection Technique. *J. Mater. Chem. B* **2014**, *2*, 7936−7944.

(24) Benjaminsen, R. V.; Mattebjerg, M. A.; Henriksen, J. R.; Moghimi, S. M.; Andresen, T. L. The Possible "Proton Sponge" Effect of Polyethylenimine (PEI) Does Not Include Change in Lysosomal PH. *Mol. Ther.* **2013**, *21*, 149−157.

(25) Subramanian, M.; Tyler, A.-J.; Luther, E.; Daniel, E.; Lim, J.; Dobson, J. Oscillating Magnet Array−Based Nanomagnetic Gene

DOI: 10.1021/acsomega.9b01000
ACS Omega 2019, 4, 12366−12374

Transfection: A Valuable Tool for Molecular Neurobiology Studies. *Nanomaterials* **2017**, *7*, 28.
(26) Oral, O.; Cıkım, T.; Zuvin, M.; Unal, O.; Yagci-Acar, H.; Gozuacik, D.; Koşar, A. Effect of Varying Magnetic Fields on Targeted Gene Delivery of Nucleic Acid-Based Molecules. *Ann. Biomed. Eng.* **2015**, *43*, 2816−2826.
(27) McBain, S. C.; Griesenbach, U.; Xenariou, S.; Keramane, A.; Batich, C. D.; Alton, E. W. F. W.; Dobson, J. Magnetic Nanoparticles as Gene Delivery Agents: Enhanced Transfection in the Presence of Oscillating Magnet Arrays. *Nanotechnology* **2008**, *19*, 405102.
(28) Lu, Y.-C.; Chang, F.-Y.; Tu, S.-J.; Chen, J.-P.; Ma, Y.-H. Cellular Uptake of Magnetite Nanoparticles Enhanced by NdFeB Magnets in Staggered Arrangement. *J. Magn. Magn. Mater.* **2017**, *427*, 71−80.
(29) Moghimi, S. M.; Symonds, P.; Murray, J. C.; Hunter, A. C.; Debska, G.; Szewczyk, A. A Two-Stage Poly(Ethylenimine)-Mediated Cytotoxicity: Implications for Gene Transfer/Therapy. *Mol. Ther.* **2005**, *11*, 990−995.
(30) Chen, Y.; Wang, W.; Lian, G.; Qian, C.; Wang, L.; Zeng, L.; Liao, C.; Liang, B.; Huang, B.; Huang, K.; et al. Development of an MRI-Visible Nonviral Vector for SiRNA Delivery Targeting Gastric Cancer. *Int. J. Nanomed.* **2012**, *7*, 359−368.
(31) Wang, X.; Zhou, L.; Ma, Y.; Li, X.; Gu, H. Control of Aggregate Size of Polyethyleneimine-Coated Magnetic Nanoparticles for Magnetofection. *Nano Res.* **2009**, *2*, 365−372.
(32) Sou, S. N.; Polizzi, K. M.; Kontoravdi, C. Evaluation of transfection methods for transient gene expression in Chinese hamster ovary cells. *Adv. Biosci. Biotechnol.* **2013**, *4*, 1013−1019.
(33) Sandbichler, A. M.; Aschberger, T.; Pelster, B. A Method to Evaluate the Efficiency of Transfection Reagents in an Adherent Zebrafish Cell Line. *BioRes. Open Access* **2013**, *2*, 20−27.
(34) Prosen, L.; Hudoklin, S.; Cemazar, M.; Stimac, M.; Lampreht Tratar, U.; Ota, M.; Scancar, J.; Romih, R.; Sersa, G. Magnetic Field Contributes to the Cellular Uptake for Effective Therapy with Magnetofection Using Plasmid DNA Encoding against Mcam in B16F10 melanoma in Vivo. *Nanomedicine* **2016**, *11*, 627−641.
(35) Cen, C.; Wu, J.; Zhang, Y.; Luo, C.; Xie, L.; Zhang, X.; Yang, X.; Li, M.; Bi, Y.; Li, T.; et al. Improving Magnetofection of Magnetic Polyethylenimine Nanoparticles into MG-63 Osteoblasts Using a Novel Uniform Magnetic Field. *Nanoscale Res. Lett.* **2019**, *14*, 90.
(36) Ouyang, S.-D.; Pei, Y. Y.; Weng, S.-P.; Lü, L.; Yu, X.-Q.; He, J.-G. Effective Polyethyleneimine-Mediated Gene Transfer into Zebrafish Cells. *Zebrafish* **2009**, *6*, 245−251.
(37) Huth, S.; Lausier, J.; Gersting, S. W.; Rudolph, C.; Plank, C.; Welsch, U.; Rosenecker, J. Insights into the Mechanism of Magnetofection Using PEI-Based Magnetofectins for Gene Transfer. *J. Gene Med.* **2004**, *6*, 923−936.

DOI: 10.1021/acsomega.9b01000
ACS Omega 2019, 4, 12366−12374